LRP 533/95 December 1995

ON LOCATING THE POLOIDAL FIELD COILS FOR TOKAMAK VERTICAL POSITION CONTROL

J.B. Lister, Y. Martin & J.-M. Moret

ON LOCATING THE POLOIDAL FIELD COILS FOR TOKAMAK VERTICAL POSITION CONTROL

J.B. Lister, Y. Martin and J-M. Moret

Centre de Recherches en Physique des Plasmas
Association EURATOM - Confédération Suisse
Ecole Polytechnique Fédérale de Lausanne
CH-1015 Lausanne

ABSTRACT

The TCV tokamak has 16 poloidal field coils for plasma shaping, distributed around the vacuum vessel. Experiments are described which determine the relative merits of the different coil positions for controlling the unstable vertical movement of elongated plasmas. The results show over an order of magnitude variation in the amplitude of the plasma vertical position response to voltages applied to the different coils. The currents induced in the vessel, the required reactive feedback power and the ohmic power dissipated in the vessel all depend strongly on the coil location. Coils on the inboard, small major radius, side of the vacuum vessel are particularly effective at producing fast vertical displacements. Comparing the results of two separate experiments with the predictions of the rigid current displacement model shows that the relative merits of the different coil positions are adequately explained by this model.

1. INTRODUCTION

Vertically elongated tokamak plasmas achieve higher performance due to an increased plasma current for given major and minor plasma radii and toroidal magnetic field. However they require active stabilisation of the inherently unstable movement of the vertical position. All elongated tokamaks have achieved this stabilisation within certain operational limits and there is an extensive literature on the modelling of vertical position control [1,2]. In large devices, the design of the feedback control of the vertical position must take into particular account three aspects of this complicated problem. Firstly, the power supplies required for poloidal field control have a high bandwidth and large inductive power, so reducing their performance requirements by appropriately designing the vertical position control would be economically important. Secondly, in the event of a loss of vertical position control, the currents induced in the vessel by the feedback control and by the plasma motion give rise to huge vertical forces in the presence of the externally applied radial fields, so reducing the magnitude of the induced vessel currents and the applied radial fields is mechanically important. Thirdly, the AC currents induced in the vessel or the surrounding structures by the flux variations associated with the vertical feedback control are significant and can give rise to unwanted or unnecessary ohmic dissipation in those elements, so reducing the eddy currents for a given feedback capability could allow greater vertical instability growth rates to be handled for a given dissipation.

A crucial design choice we must make for improving these aspects is the physical location of all of the poloidal field coils and the distribution of the control voltages between them. In prior work it was shown that the poloidal location of the coils used for vertical position control had a significant effect on vertical controllability. Improvements in the vertical position control of the DIII-D tokamak arose from an optimisation based on these considerations and allowed operation up to an elongation of 2.5, close to the limit achievable in the DIII-D vacuum vessel [2,3]. This paper will show that it is possible to reduce significantly the required inductive power, the vacuum vessel eddy currents and their associated dissipation, supported by a simple model of the vertical position control. However, in opposition to choosing the poloidal coil locations freely, we find many practical constraints of access to the torus, its assembly and maintainance, as well as restrictions on the usage of space in the inner column of the tokamak. The design of any specific machine involves a difficult trade-off between all of these considerations. In addition, this trade-off is influenced by a priori appreciations of the performance of the machine; for example via confinement scaling laws which are all notoriously weak in determining the performance as a function of the plasma geometry, particularly the toroidal aspect ratio.

The control of the vertical position is a sensitive task in plasma shape control, since it alone is unstable. It can usefully be separated from the general problems of shape control for two reasons. Firstly, the frequency bandwidth and the required feedback voltages are imposed by the growth rate of the vertical position instability and by the variation in the plasma vertical position which must be controlled, rather than by a choice of operational time-scales. Shape and current control can always be slowed down to stay within the limits of the poloidal field supplies, whereas the vertical position control cannot. In present devices, shape control is usually performed on a slower time-scale than the time-constants of the vessel current distribution. Secondly, the vertical position control is only weakly dependent on the plasma equilibrium model but depends strongly on the spatial structure of the radial field produced by up-down anti-symmetric shaping current distributions. On the other hand, the equilibrium model is critical in determining the reaction of the plasma to applied vertical field. We can therefore usefully consider the action of up-down anti-symmetric coil currents/voltages to be almost independent of the plasma model whereas up-down symmetric coil currents/voltages couple strongly to the plasma shape and we require a full plasma equilibrium model to simulate their effect. This separation is strictly true for up-down symmetric shapes.

In this paper we present systematic measurements of the relative merits of up-down anti-symmetric pairs of coils, located at different poloidal positions, for controlling the vertical position of up-down symmetric plasmas in the TCV tokamak. Two different experiments and their results are presented in Section 2, showing the effect of the coil-pair position on the amplitude and speed of the plasma position response, the currents induced in the vacuum vessel and their ohmic dissipation. The measurements are all made and discussed in terms of the response of the plasma vertical position, measured with the vertical position feedback loop closed, an approach justified in Appendix A. In order to understand the large differences between the responses to excitation by different coil-pairs, we model the plasma vertical position movement using a rigid current displacement model (RCDM). Simulating the exact experimental conditions allows us to compare the model predictions with the experimental results, Section 3, and to understand the influence of the poloidal location of the control coils. Section 4 concludes with a discussion of the results.

2. EXPERIMENTAL RESULTS

2.1 General Conditions

TCV (Tokamak à Configuration Variable) was constructed to explore the detailed effects of shape on plasma performance. The design of TCV is up-down symmetric, Fig. 1, and its constructional parameters are : R = 0.88m, a = 0.24m, height = 1.44m, B_ϕ = 1.43T. To be freely capable of producing widely different configurations, TCV is equipped with a set of 16 independently powered poloidal shaping coils, eight in a vertical stack on each side of the vacuum vessel. The vessel itself has an almost rectangular aperture with a height/width ratio of 3.0. It has an irregular shape and varying thickness with the poloidal distribution of electrical conductivity concentrated in the top and bottom plates. The electro-magnetic properties of the vacuum vessel are described in this paper by a set of eigenmodes, obtained by a general diagonalisation of the mutual inductances and resistances of 512 filaments modelling the vacuum vessel. The slowest up-down symmetric and anti-symmetric eigenmodes have decay time-constants of 13.4 and 8.1 msec. respectively.

Figure 1 also shows the diagnostic measurements available for plasma shape control, namely a set of poloidal field pick-up coils inside the vessel and a set of poloidal flux loops. Different methods have already been tested for real time discharge control, using the flexible hybrid analog-digital TCV Plasma Control System [4]. The shapes so far produced in TCV cover a wide range of current, elongation and triangularity, including limited and diverted discharges with upper and lower Single-Nulls and Double-Nulls. The achieved plasma currents extend up to 810 kA, the elongations to 2.05 and the triangularity varies from - 0.7 to 0.8 [5,6]. In the discharges used in this paper, all plasma shape parameters, with the exception of the vertical position, were controlled using a set of heuristic combinations of the poloidal flux and poloidal field measurements. The reference waveforms for these combinations were programmed using a Neural Network [7]. We have implemented several plasma vertical position observers on TCV including simple up-down flux-loop differences, up-down extrapolated flux-loop differences and poloidal field moments [5]. For the work described in this paper we have used an observer of the current-weighted vertical plasma position, $z(t)I_p(t)$, hereafter referred to as zI_p. We use the current-weighted plasma vertical position zI_p since it is linearly related to any applied poloidal flux variation. We approximate the desired form of the contour integral by the expression :

$$\mu_0 zI_p = \sum_{i=1}^{38} z_i Bpol_i \delta l_i + \sum_{i=2}^{38} \Delta\psi_i \beta_i \sim \int\{z B_{//}+Rlog(R/R_0)B_\perp\}dl \qquad (2.1)$$

in which z_i and δl_i are the vertical position and the spacing between the 38 poloidal magnetic field measurements, $Bpol_i$, and $\Delta\psi_i$ are 37 flux-loop differences with respect to the poloidal flux at the vessel mid-plane on the inner side. β_i is a set of coefficients

chosen to produce minimum contributions of the individual poloidal field coil currents to the zI_p observer in the absence of any plasma current. zI_p is compared in real time with a pre-programmed reference waveform $z_{ref}(t)$ multiplied in real time by the measured value of $I_p(t)$. This form of reference programming is preferred to programming a pure reference value of zI_p directly, since the latter produces an apparent vertical position error in the presence of a plasma current error.

Having created the observers for shape and position parameters, we must correct the poloidal coil currents for the errors in these control parameters and subsequently determine the timescales on which these corrections must be applied. This is done differently for the shape parameters and the vertical position. For the shape parameters, the distribution of correction currents among the different shaping coils, $\delta\mathbf{I}_{pol}$, is estimated as the inverse of the observer sensitivity matrix, derived with no plasma current and no vessel currents:

$$\delta\mathbf{I}_{pol} = \left(\mathbf{A} \cdot \frac{\partial[\,\mathbf{B}_{pol},\,\Delta\psi]}{\partial\,\mathbf{I}_{pol}}\right)^{-1} \cdot \varepsilon_{CP} \qquad (2.2)$$

where A is the matrix creating the heuristic shape parameters from the input signals, [$\mathbf{B}_{pol}$, and $\Delta\psi$]. (Bold type indicates a vector of signals throughout and open-type indicates a matrix). ε_{CP} is the set of errors in the heuristic control parameters. This simple method produces a shape controller which is independent of the plasma equilibrium and which only depends on the definition of the particular linear shape parameters to be controlled. Although this procedure leads to strict decoupling between the separate shape control parameters only in the absence of plasma, the decoupling actually obtained in the presence of a plasma is excellent.

The feedback controller for the dynamic correction of the poloidal shaping currents is of the form :

$$\delta\dot{\mathbf{I}}_{pol} = \left[\mathbf{P} \cdot \mathrm{diag}\left(\frac{1}{\tau_P}\right) + \mathbf{I} \cdot \mathrm{diag}\left(\frac{1}{s\cdot\tau_I\tau_P}\right) + \mathbf{D} \cdot \mathrm{diag}\left(s\cdot\frac{\tau_D}{\tau_P}\right)\right] \cdot \varepsilon_{CP} \qquad (2.3)$$

For all the shape parameters excluding the vertical position, the matrices P, I, and D are the same, derived as in Equation (2.2). and their feedback time-constants are the same. τ_P defines the timescale of the proportional correction of the feedback error, τ_D defines the relative importance of the derivative feedback and τ_I defines the timescale on which integral errors are cancelled.

For the control of the vertical position, such a simple method is inapplicable since the observer defined in Equation (2.1) is specifically constructed to be independent of the control coil currents in the absence of plasma, contrary to the case of the shape parameters which allowed the use of Equation (2.2). We calculate the necessary radial field correction assuming a typical vertical field curvature and apply this correction using many poloidal field coils, distributing the correction current requests between them intuitively on the basis of previous modelling [2]. Proportional and derivative feedback are applied to the coil-pairs E2-E7, E3-E6, E4-E5, F2-F7,F3-F6 and integral feedback is applied to the coil-pairs F1-F8, F2-F7, E1-E8 and E2-E7. We use weak integral feedback (τ_I ~ 100 msec) to ensure that a zero position offset is obtained with finite proportional gain (τ_P ~ 20 msec). Derivative feedback (τ_D ~ 1 msec) produces vertical stabilisation and the damping of vertical position control oscillations.

Vertical position control has already stabilised TCV plasmas with growth rates up to 800 sec^{-1} [5]. The power supply bandwidth, limited by a 1 msec thyristor switching time, has so far prevented us from exceeding this value. In order not to suffer from the limited bandwidth of the power supplies, the experiments in this paper were performed with the following limiter plasma parameters : B_ϕ=1.43T, I_p = 200kA, δ=0.21, κ=1.45, q_a=4.6, the plasma current being centred in the vessel as shown in Fig. 1. The estimated growth rate for these plasmas is 290 sec^{-1}. All conditions were held essentially constant for 0.7 seconds in the plasma pulse.

2.2 The Perturbative Method

The vertical movement of the plasma can be studied experimentally in several ways. The simplest is to open the control loop and measure the ensuing unstable vertical motion. This has the disadvantage of leading to a disruption as well as non-linearity problems as the excursion increases. Stimulating the closed feedback loop by injecting perturbation signals into the loop is an alternative method. In the work described perturbations are directly summed into the voltage demand signals for the poloidal field coil supplies, shown as the inputs $\mathbf{g}$ in a simplified block diagram, Fig. 2. In this case we measure the response of the loop to a perturbation, not its response to a change in the reference signal. Comparing the responses of different coils in this manner in fact gives the same result as comparing the open loop responses, demonstrated in Appendix A. Injecting perturbations into the closed feedback loop indicates which coils are able to provoke a significant vertical movement for different frequencies. Those coils which provoke the smallest movement at high frequency are likely to be those which are least useful for controlling the unstable vertical position.

We have carried out perturbation excitation for all eight up-down anti-symmetric pairs, such as E8-E1, F5-F4, Fig. 1. Two types of perturbation have been applied, square-wave injection and continous random injection; the experiments are described separately. Since both methods excite the same points in the feedback loop, the experiments are essentially the same, in that the same information could be extracted from both. In practice, the spectral content of the continuous excitation is fairly flat out to 250 Hz and should provide more information for a given excursion of the controlled parameter. Continuous stimulation of the closed feedback loop should also allow us to monitor the dynamics of the open loop system being controlled, although such an analysis is not the aim of this present paper. Similar continuous excitation experiments have been carried out on the COMPASS-D tokamak to quantify the feedback loop performance [8].

2.3 Square-Wave Excitation

In the first experiment, we successively excited each up-down anti-symmetric coil-pair within a single tokamak discharge, applying single 25 msec. pulses of opposite signs to the upper and lower coils simultaneously. Figure 3 shows the time-history of the voltage perturbations (**Q**), the demand signals and perturbations summed (**U**, Fig. 2), the coil currents and the plasma position response (zI_p, Fig. 2). The asymptotic response of the feedback loop to these perturbations is to annul them in the presence of integral feedback gain, since only a step in a reference input should lead to a step in a controlled parameter. However, the time-scale of the perturbations is such that the feedback loop does not have time to annul them completely, although the tendency is visible in the figure. This is not a problem for us, since we are essentially looking for responses on the timescale of the vessel current decay and faster.

Up-down anti-symmetric excitation provides a zero net poloidal flux perturbation and does not couple to the total plasma current. Its measured effect on all shape parameters other than the vertical position was negligible for the reasons invoked in the introduction, confirming the simplicity of this experiment.

The differences between the responses of the different coil-pairs are striking, considering that the coil-pairs were excited by the same perturbation with similar volt-seconds injected. The responses for the coil-pairs F8-F1 and E8-E1 are particularly damped, indicating that these coils will not be able to provide fast recuperation of jumps in the vertical position, nor will they be able to stabilise the most unstable plasmas. The coil-pairs E6-E3 and E5-E4 show significant overshoot in the response, indicating a

faster penetration of the radial control flux. The coils which provide both the fastest and largest experimental responses are those already used in the vertical position feedback loop itself.

The square-wave injection response provides a nice visualisation of the coil-pair responses for comparison with a modelled response. The frequency spectrum of this type of perturbation is rather poor for a given amplitude of the position excursion. The method used in the following section presents an alternative for quantifying the response.

2.4 Random Excitation

In the second experiment, a random binary sequence continuous excitation was injected into the same points in the feedback loop as in the case of the square-wave injection (inputs **Q**). In this method, a random time-sequence of either +U or -U volts was applied to the two coils in each coil-pair, in opposition, for a duration of 700 msec. The time-step of the random sequence was 1 msec, interpolation between points being linear. This procedure was repeated one coil-pair at a time over a series of eight identical stationary discharges with the same random excitation sequence used for all coil-pairs. Coupling to the current and all shape parameters other than the vertical position was measured to be negligible, as for the square-wave excitation.

Figure 4 shows the time-response of the current-weighted plasma vertical position which is linearly related to the applied flux perturbation. Its standard deviation, $\sigma(zI_p)$, is also indicated for each coil-pair. Before and after the perturbation injection there is a residual $\sigma(zI_p)$ of about 60 A.m. A similar experiment was carried out with simultaneous injection into all coil-pairs, but this time injecting non-correlated random sequences into each coil-pair. $\sigma(zI_p)$ was measured to be 1897 A.m, close to the $\sigma(zI_p)$ calculated from the separate excitations, 1832 A.m, illustrating that we can achieve effective decorrelation of the noise injection within 700 msec. Increasing and decreasing the amplitude of these simultaneous injections by a factor two verified the linearity of the response. The different amplitudes of the responses are clear, but the nature of the response, overshoot or damped, is not visible in the raw data, as it was for the square-wave injection.

$\sigma(zI_p)$ varied widely from coil-pair to coil-pair over a range 165 - 1213 A.m, tabulated in Column 1 of Table I and shown in Fig. 5(a) with the coil-pairs plotted ordered around the vessel. The response is even slightly overstated due to the 60 A.m residual variation without excitation. The smallest response was obtained for the coil-pair F8-F1. The outer

stack coil-pair F7-F2 and the extreme inner stack coil-pair E8-E1 are also fairly weakly coupled to the plasma vertical position. The coil-pairs which provided the largest $\sigma(zI_p)$ response, E6-E3, E5-E4 and F6-F3 also provided the largest and fastest pulse-response in the first experiment.

Column 2 of Table I and Fig. 5(b) summarises the effective reactive power requirement for the individual coil-pairs, needed to excite a unit vertical position movement (1 A.m) with the voltage perturbation flat as a function of the excitation frequency. This quantity is evaluated combining the standard deviation of the coil-pair currents and voltages: $\sigma(U)\sigma(Ipol) / \sigma^2(zI_p)$. The variation between the reactive power used for the in-board and out-board coils is less than the variation in their $\sigma(zI_p)$ responses for fixed applied voltages due to their different inductances, but the hierarchy already established is maintained.

We have analysed the poloidal distribution of the vessel currents from the poloidal distribution of the loop voltage measured using the 38 voltage loops placed on the outer surface of the vessel, combined with a constructional estimate of the poloidal distribution of the vacuum vessel resistivity. Figure 6 shows the poloidal distribution of these currents, illustrating their closeness to the driven coils as to be expected. Table I column 3 shows the values of the ohmic power dissipated in the whole vessel, Fig. 5(c), normalised for $\sigma(zI_p)$ = 1 A.m. The ohmic power dissipated in the vacuum vessel for a given vertical plasma displacement varies by a factor of 10 between the F1-F8 combination, the worst, and the E6-E3 combination, the best. Changing the coils used for the vertical feedback control therefore has a factor of 10 effect on the power dissipated in the vacuum vessel, or has a factor of Ã10 on the amplitude of the excursion which can be controlled given limited feedback power.

2.5 Resume of the Experimental Information

These two experiments carried out on TCV have shown that there is a significant difference between the reaction of the plasma vertical position to voltage excitation of the different up-down anti-symmetric poloidal field coil-pairs. In order to understand the underlying mechanism determining this difference between coil-pairs, we inspect the predictions of a model of the vertical plasma movement based on simple considerations of the movement of a rigid but distributed plasma current.

3. MODELLING OF THE RESULTS

3.1 The Rigid Current Displacement Model

A simple rigid current displacement model describing the interaction between a centred filamentary plasma with a single active anti-symmetric poloidal coil in the presence of a single vacuum vessel eigenmode was applied earlier to the DIII-D tokamak [2]. This model remains attractive by its simplicity and its similarity to experimental observations, as well as to its ability to predict good vertical position feedback controllers [3]. However, we have had to extend this model in several directions for application to TCV.

Firstly, the design of the TCV vacuum vessel together with the fact that the plasma current may not be centred vertically leads to time constants of the vacuum vessel current distribution eigenmodes which are poorly separated. As a result we take the slowest 20 eigenmodes of the vessel into consideration, including up-down symmetric and up-down anti-symmetric modes. All conducting structures in which toroidal current can be induced during vertical position control can be included into this eigenmode decomposition, although TCV does not need this complication.

Secondly, we wish to treat the system with all the coils active together rather than modelling separate coil-pairs on their own. This is done by explictly including all poloidal field shaping coils in the circuit equations as eight anti-symmetric pairs.

Thirdly, in the face of the highly structured vacuum equilibrium field possible for TCV plasmas, we perform a volume integration of the forces on the plasma due to the radial fields from the vacuum vessel currents and the coil-pair currents. This does not alter the structure of the control problem and we find that it does not change the estimate of the growth-rate, provided the radial position of the current filament is taken as the major-radius-weighted value of the current distribution, $\langle R_{fil} \rangle = \int j(\mathbf{r})\, R(\mathbf{r}) d^2\mathbf{r} \,/\, I_p$.

The feedback of the vertical position error $\varepsilon(zI_p)$ is added to the model as a vector of voltage corrections (Fig. 2): $\mathbf{U}_{fb} = M_{aa} \bullet (1/s\, \mathbf{G}_i + \mathbf{G}_p + s\mathbf{G}_d) \bullet \varepsilon(zI_p) = (1/s\, \mathbf{C}_i + \mathbf{C}_p + s\mathbf{C}_d) \bullet \varepsilon(zI_p)$, where $\mathbf{G}_i$, $\mathbf{G}_p$ and $\mathbf{G}_d$ are the vectors of gain values actually used in the discharges to be modelled and M_{aa} is the mutual inductance matrix for the poloidal field coils. In order to model the integral feedback term, we add an extra variable, representing the time-integral of the error signal. Including this term led to much better agreement between the experimental results and the model.

Finally we must make a first approximation for the power supply response. The necessity for this is obvious from the almost square response of the coil-pair currents to the voltage input signals, Fig. 3, indicating an apparent resistive load for frequencies at which the coils themselves are mostly inductive. This correction is due to the control mode of the power supplies as they were used in these particular experiments. The external voltage demand input signal is internally in opposition to a proportional controller maintaining the coil current close to a pre-programmed current demand input signal. The weak gain in this internal power-supply controller corresponds exactly to an additional effective resistance, $R_a \dashrightarrow R_a + K$ where $K = 2x0.51\ \Omega$ and $2x3.24\ \Omega$ for the E- and F-coil-pairs respectively.

We presuppose that the only voltage demand inputs to the power supply pairs arise from the zI_p feedback controller **C**(s). In practice, the other feedback loops controlling the plasma shape are also active and would produce a control loop response if their errors were sensitive to the zI_p error. To first order there is no coupling for the up-down symmetric shape control used in these discharges, as already discussed.

With all of these modifications, the set of differential equations describing the plasma current vertical position, the vessel eigenmode currents and the coil-pair currents and voltages becomes :

$$\begin{bmatrix} s M_{aa} + R_a & s M_{ae} & s\frac{\partial M_{ap}(z)}{\partial z} + s C_d + C_p & C_i \\ s M_{ae}^{T} & s M_{ee} + R_e & s\frac{\partial M_{ep}(z)}{\partial z} & 0 \\ -s\frac{\partial M_{ap}(z)}{\partial z} & -s\frac{\partial M_{ep}(z)}{\partial z} & -s\bullet\frac{\left(\frac{\partial M_{ep}(z)}{\partial z}\right)^2}{L_e}\frac{\alpha(z,I_{pol})}{\alpha_{crit}} & 0 \\ 0 & 0 & -1 & s \end{bmatrix} \begin{bmatrix} I_a \\ I_e \\ z\,I_p \\ \int z\,I_p\,dt \end{bmatrix} = \begin{bmatrix} Q \\ 0 \\ 0 \\ 0 \end{bmatrix} \qquad (3.1)$$

where I_e, M_{ee}, $\partial M_{ep}/\partial z$ and R_e are the vessel eigenmode currents, their mutual inductances, their mutual inductance with the vertical position and their resistances; I_a, M_{aa}, $\partial M_{ap}/\partial z$ and R_a are the same for the active shaping coil-pairs; L_e is the self-inductance of the vessel eigenmodes; Mae is the mutual inductance matrix between the vessel eigenmodes and the coil-pairs; the term α/α_{crit} defines the stability margin F_{stab}/F_{destab}, where α_{crit} defines the maximum value of field curvature for which the

vertical position is stable in a perfectly conducting vessel. It corresponds to the limit as the determinant of Equation (3.1) approaches zero. The mutual inductances between the currents and the plasma vertical position was calculated for a filamentary current in [2] and we have calculated these values by integrating the coupled flux over the plasma cross-section and differentiating with respect to a displacement of the current distribution itself. All electro-magnetic properties of TCV are derived from the geometry of TCV rather than from physical measurements.

The destabilising force due to the imposed field curvature, $\partial B_R/\partial z$, is given by :

$$F_{destab} = \delta z \int j(\mathbf{r}) \frac{\partial B_R(\mathbf{r})}{\partial z} \, d^3\mathbf{r} \qquad (3.2)$$

where $B_R(\mathbf{r})$ is the radial equilibrium field and δz is a vertical displacement. The image currents induced in the vessel are given by the amplitudes of their eigenmodes:

$$I_{ek} = \delta z \int j(\mathbf{r}) \frac{\partial B_{Rek}(\mathbf{r})}{\partial z} \, d^3\mathbf{r} \qquad (3.3)$$

and give rise to a stabilising force :

$$F_{stab} = \int j(\mathbf{r}) \sum_k \frac{\partial B_{Rek}(\mathbf{r})}{\partial z} I_{ek} \, d^3\mathbf{r} \qquad (3.4)$$

where $B_{Rek}(\mathbf{r})$ is the radial field produced by a unit current in the kth vessel eigenmode. We prefer the form α/α_{crit} in Equations (3.1) to the previously used form involving the poloidal field curvature index since the former does not depend on the equilibrium vertical field which has no role in the vertical stabilisation.

3.2 Required number of eigenmodes in the model

With the feedback gains in Equations (3.1) set to zero, these equations determine the poles of the open loop system. With one vessel eigenmode there are 9 non-zero poles. As we gradually increase the number of vessel eigenmodes considered in Equations (3.1), the poles derived from the equations are displaced, but they finally settle, as seen in Fig. 7. Only one of the poles is unstable, by the structure of Equations (3.1). The number of eigenmodes necessary to describe the plasma motion up to poles faster than the 1 msec switching time of the thyristor power supplies is 20.

3.3 Comparison of the RCDM with the Square-Wave Injection

Equation (3.1) can be used to model the response of the plasma vertical position to arbitrary and multiple input waveforms by time-integration. Eight input pulses were injected during a single simulation, exactly as in the experiment, Fig. 3, and the result is shown as a dotted-dashed line in Fig. 8, overlaying the experimental signal, shown as a solid line. The rather damped experimental responses of coil-pairs E1-E8 and F1-F8 are well reproduced. The fast experimental responses with significant overshoot, coil-pairs E6-E3 and E5-E4, are also well modelled. This excellent agreement implies that the underlying mechanisms determining the zI_p evolution are contained in Equations (3.1), specifically, the large differences between the effectiveness of the various coil-pairs already seen in Fig. 3 is faithfully reproduced.

3.4 Comparison of the RCDM with the Random Injection

We evaluated the modelled time-response to the random injection in the same manner and calculated its standard deviation. However, the random injection has a fairly flat voltage frequency spectrum and for each coil-pair we therefore expect $\sigma(zI_p)$ to be given by : $\sigma^2(zI_p) \sim \sum_k H^2_{QiZ}(\omega_k)$. These two methods of evaluating the modelled response agreed. Figure 9 shows the values of the modelled response for the eight coil-pairs, adding a 60 A.m. residual amplitude, plotted against the experimental responses $\sigma(zI_p)$ taken from Fig. 4. The agreement is excellent.

4. DISCUSSION

The very simple experiments described in this paper have demonstrated a large variation in the quality of the plasma vertical position response to different forms of voltage perturbation applied to up-down anti-symmetric coil-pairs in TCV. These different responses were compared with the vertical position feedback loop closed, avoiding the necessity of evaluating the less accessible open-loop responses. The results clearly show the extreme importance of the poloidal location of the vertical feedback control coils. We can reduce the reactive power, reduce the power dissipation leading to vessel heating or

reduce the image currents in the vessel by choosing the coil positions used for the control of the vertical position according to these experimental results.

The coil-pairs F1-F8 and E1-E8 provide a large radial field on axis for a given current, Column 4 of Table I. However they also couple strongly to the slowest up-down anti-symmetic eigenmode of the vacuum vessel, Column 5 of Table I. The slow vessel eigenmodes, whose amplitudes peak at the top and bottom of the TCV vessel, effectively shield the radial magnetic field generated by these coil-pairs. The coil-pairs which are best coupled to the fast vertical motion are those in the inner stack close to the equatorial plane, providing relatively weak radial magnetic field on axis, namely E6-E3 and E5-E4. However, since they are also weakly coupled to the slow vacuum vessel eigenmodes, these coil-pairs allow faster action on the plasma position. The distance of the coil from the plasma axis, Table I Column 6, does not alone determine the amplitude of the response either.

These findings give us confidence to use the RCDM as the basis for the construction of optimised feedback control laws, provided that the frequency response is also correctly modelled. The next step, to derive the full frequency response of the closed vertical feedback loop to the chosen perturbation injection from these data, or from new experiments deisgned with this goal in mind, will be the object of further study.

In order to generalise these experimental results, we have modelled the response of a simple rigid current displacement and find that it contains the salient features of the plasma vertical movement. The optimisations necessary for future devices can therefore usefully be performed using this model.

We have used the model to calculate the values of α/α_{crit} which can be stabilised by each coil-pair acting on its own, Fig. 5(d), done by exploring the closed loop stability for different controller gains. The coils which provide the slowest response also have the lowest stabilisation limits, confirming the results of [2,3].

The advantages measured when using poloidal field coils on the small major radius side of the torus suggest that significant reductions in the required power, induced currents and unwanted AC ohmic losses in the vessel and surrounding structure can be achieved. The cost would be a very small increase in the aspect ratio. Such inboard vertical control coils would need to carry no DC shaping current and their power handling and physical size should not cause problems. As cited in the introduction, such design considerations depend on our weak understanding of the trade-off between major radius and aspect ratio in determining final plasma performance. The agreement between

the TCV results and the simple RCDM suggest that such an optimisation can be realistically carried out for any new geometry to confirm these findings.

ACKNOWLEDGEMENTS

It is a pleasure to acknowledge the collaboration of the TCV team in these measurements. We are grateful for stimulating discussions with Mike Browne of JET, Dominique Bonvin of the EPFL and Ed Lazarus of ORNL. This work was partially supported by the Fonds National Suisse pour la Recherche Scientifique.

APPENDIX A. THE CLOSED LOOP RESPONSE TO PERTURBATIONS

The responses of the closed feedback loop system to the external voltage perturbations which are discussed in this paper are the time-domain response to pulse injection, the standard deviation of the amplitude of the response to continuous random excitation and the response as a function of frequency. These do not directly measure the unstable characteristic of the system to be controlled. If we were to change the feedback controller gains, the responses measured would change. We must therefore ask whether these responses are of general significance, or whether they are mainly a property of the controller with which the feedback loop is closed, or even of the growth rate of the vertical instability itself.

In order to address this question we refer to the simple diagram of the feedback loop, Fig. 2, in which we have assumed that there is only one output variable, the plasma position, and that the vector controller $\mathbf{C}(s)$ has 8 voltage outputs and the tokamak (including the power supplies) $\mathbf{T}(s)$ has 8 voltage inputs, which are being individually controlled. The transfer function from the inputs $\mathbf{Q}$ to the single output zI_p is defined as:

$$zI_p(s) = \mathbf{H}_{QZ}(s) \bullet \mathbf{Q}(s) \ ,$$

with $$(1 + \mathbf{T}(s) \bullet \mathbf{C}(s)) \, zI_p(s) = \mathbf{T}(s) \bullet \mathbf{P}(s) \ ,$$

we obtain $$zI_p(s) = (1 + \mathbf{T}(s) \bullet \mathbf{C}(s))^{-1} \bullet \mathbf{T}(s) \bullet \mathbf{Q}(s) \ ,$$

and so $$\mathbf{H}_{QZ}(s) = (1 + \mathbf{T}(s) \bullet \mathbf{C}(s))^{-1} \bullet \mathbf{T}(s) \qquad (A.1)$$

The individual transfer functions $\mathbf{C}(s)$ and $\mathbf{T}(s)$ may be expressed explicitly as polynomial ratios $B(s)/A(s)$. The dynamics of the controller denominator, $A_C(s)$, are identical by design of the controller hardware. The open-loop system $\mathbf{T}(s)$ has numerators

$B_{TI}(s)$ which are dependent upon the input being stimulated and a denominator $A_T(s)$ which is common to all inputs. We can therefore re-express (A.1) as :

$$H_{QIZ}(s) = B_{TI}(s)\, A_C(s) \;/\; \left(\sum_{j=1}^{8} B_{Cj}(s)\, B_{Tj}(s) + A_C(s)\, A_T(s) \right) \qquad (A.2)$$

The denominator of the closed-loop response, $\sum_{j=1}^{8} B_{Cj}(s)B_{Tj}(s) + A_C(s)A_T(s)$, is common to all of the responses and defines the poles of the response of zI_p to the perturbation voltage. The input-dependent part of the closed-loop system numerator is therefore demonstrated to be the same as the input-dependent part of the open-loop system numerator. Comparing the responses of the different coil-pair inputs in the experiments described is therefore equivalent to comparing the input-dependent numerators of the controlled system, without the disadvantages of having to open the feedback loop. The result is therefore guaranteed to be independent of the controller used in the feedback loop.

REFERENCES

[1] PERRONE,M.R. and WESSON,J.A., Nuclear Fusion **21** 871 (1981)
JARDIN,S.C. and LARRABEE,D.A., Nuclear Fusion **22** (1982)
HUTCHINSON,I.H., Nuclear Fusion **29** 2107 (1989)
WARD,D.J. and JARDIN,S.C., Nuclear Fusion **32** 973 (1992)
HUMPHREYS,D.A. and HUTCHINSON,I.H., Fusion Technology, **23** 167 (1993)
WARD,D.J., BONDESSON,A. and HOFMANN,F., Nuclear Fusion **33** 821 (1993)
WARD,D.J. and HOFMANN,F., Nuclear Fusion **34** 401 (1994)

[2] LAZARUS,E.A., LISTER,J.B. and NIELSON,G.H., Nuclear Fusion, **30**, 111 (1990)

[3] LISTER,J.B., LAZARUS,E.A., et al. Nuclear Fusion, **30**, 2349 (1990)
LAZARUS,E.A., CHU,M.S. et al., Phys. Fluids B, 2220 (1991)

[4] ISOZ,P.F., LISTER,J.B., MARMILLOD,Ph., Proc 16th Symp on Fusion Technology, Oxford, 1990 1264 (1991)

[5] HOFMANN,F., LISTER,J.B. et al., Plasma Phys. and Contr. Fusion, **36**, B277 (1994)

[6] LISTER,J.B., HOFMANN,F. et al., 15th Int. IAEA Conf. on Plasma Phys. and Contr. Nucl. Fusion, A-5-1-2, Seville (1994)

[7] LISTER,J.B., MARTIN,Y. and MORET,J-M., 21st EPS Conf. on Contr. Fusion and Plasma Phys., Montpellier (1994)

[8] VYAS,P., MORRIS,A.W. and MUSTAFA,D., Proc. 18th Symposium on Fusion Technology, Karlsruhe, 1994 (1995)

[9] LJUNG,L. System Identification, Prentice-Hall (1987)

[10 MORET,J-M. Lausanne Report LRP 498/94 (1994)

FIGURE CAPTIONS

1. The construction of TCV showing the poloidal field coil labelling, the position of the flux-loops (marked x on the vessel) and field probes (marked - inside the tiles). The plasma shown (# 6710) is the weakly-shaped limited plasma used in these experiments, with the following parameters : B_ϕ=1.43, I_p = 200kA, δ=0.21, κ=1.45, q_a=4.6.

2. Simple figure of the vertical position feedback control loop, showing the 8 anti-symmetric voltage demand signals (**U**) and perturbation inputs (**Q**). The transfer functions of the SIMO feedback controller, **C**(s), and that of the MISO comprising power supplies (PS) plus plasma-vessel-coil system, **T**(s), are also indicated.

3. Response of the system to square-wave pulse injection. For each anti-symmetric coil-pair we show the perturbation (Q), the voltage demand (U) and the coil-pair current (I). The vertical position zI_p is also shown.

4. Plasma position response to 700 msec. of continuous anti-symmetric excitation by a random binary sequence for each of the 8 TCV coil-pairs. The variation of the current-weighted vertical plasma position response is indicated for each coil-pair (RMS).

5. The response of TCV to random continuous anti-symmetric perturbation of different coil-pairs. The coils are ordered according to their poloidal position, Fig. 1. a) standard deviation of the vertical position response; b) Reactive power for unit modulation; c) Total ohmic dissipation in the vessel; d) Maximum field curvature for which the RCDM predicts vertical stabilisation using only that coil-pair, expressed as α/α_{crit}.

6. Measured poloidal distribution of the induced vessel currents during the square-wave injection.

7. Evolution of the real open-loop poles as the number of eigenmodes in the vessel description is increased. Adding up-down symmetric eigenmodes to the centred plasma used in the model does not change the system response, explaining the step-wise evolution of the poles.

8. Comparison between the experimental square-wave response (solid line) and the modelled square-wave response (dotted-dashed line) of the zI_p position.

9. Comparison between the modelled and measured $\sigma(zI_p)$ position responses for the eight coil-pairs.

Table I.

Continuous random injection experiments for all coil-pairs: 1) $\sigma(zI_p)$ for +-200 Volt excitation on each coil-pair; 2) Reactive power in the coil-pair for a unit RMS displacement; 3) Power dissipated in the vacuum vessel for unit $\sigma(zI_p)$; 2) Radial field on axis per unit coil-pair current; 5) Coupling coefficient between the coil-pair and the slowest anti-symmetric eigenmode of the vessel; 6) Inverse separation of the coil currents from the magnetic axis.

	1	4	5	6	2	3
Coil-Pair	$\sigma(zI_p)$	B_R $T*10^6$	k-mut	1./sep m^{-1}	VA VA	P_{oh} W
E5-E4	945	32	0.11	2.6	0.21	0.005
E6-E3	1213	57	0.25	2.1	0.11	0.004
E7-E2	612	46	0.37	1.6	0.42	0.008
E8-E1	274	32	0.43	1.3	2.0	0.038
F8-F1	165	59	0.45	1.1	3.1	0.032
F7-F2	255	71	0.47	1.3	1.3	0.017
F6-F3	543	78	0.32	1.9	0.29	0.005
F5-F4	393	52	0.19	2.2	1.0	0.007

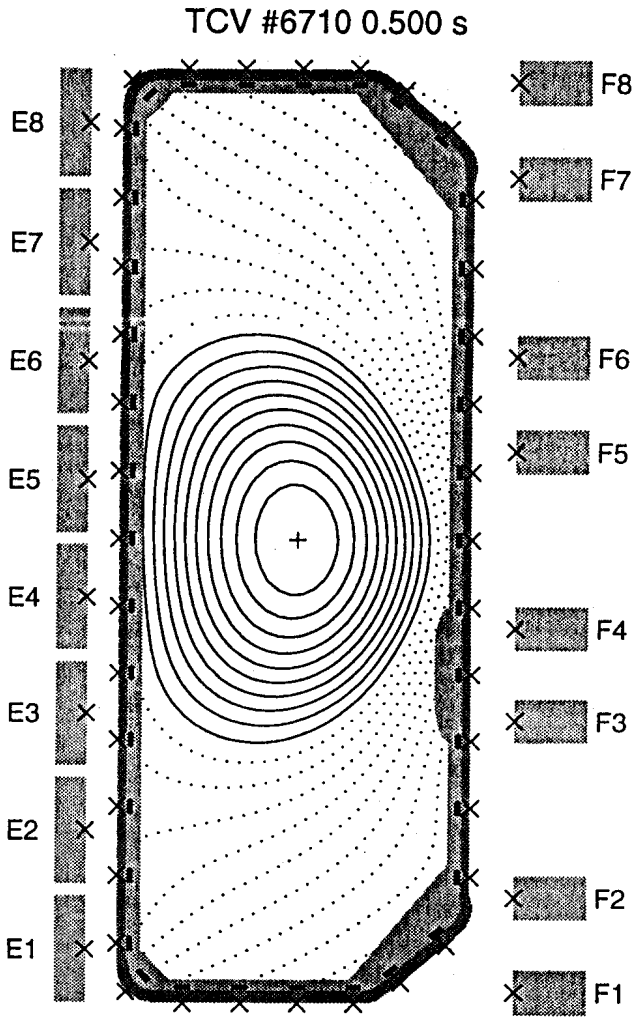

1. The construction of TCV showing the poloidal field coil labelling, the position of the flux-loops (marked x on the vessel) and field probes (marked - inside the tiles). The plasma shown (# 6710) is the weakly-shaped limited plasma used in these experiments, with the following parameters : B_ϕ=1.43, I_p = 200kA, δ=0.21, κ=1.45, q_a=4.6.

Perturbation injection into the TCV Plasma Control System

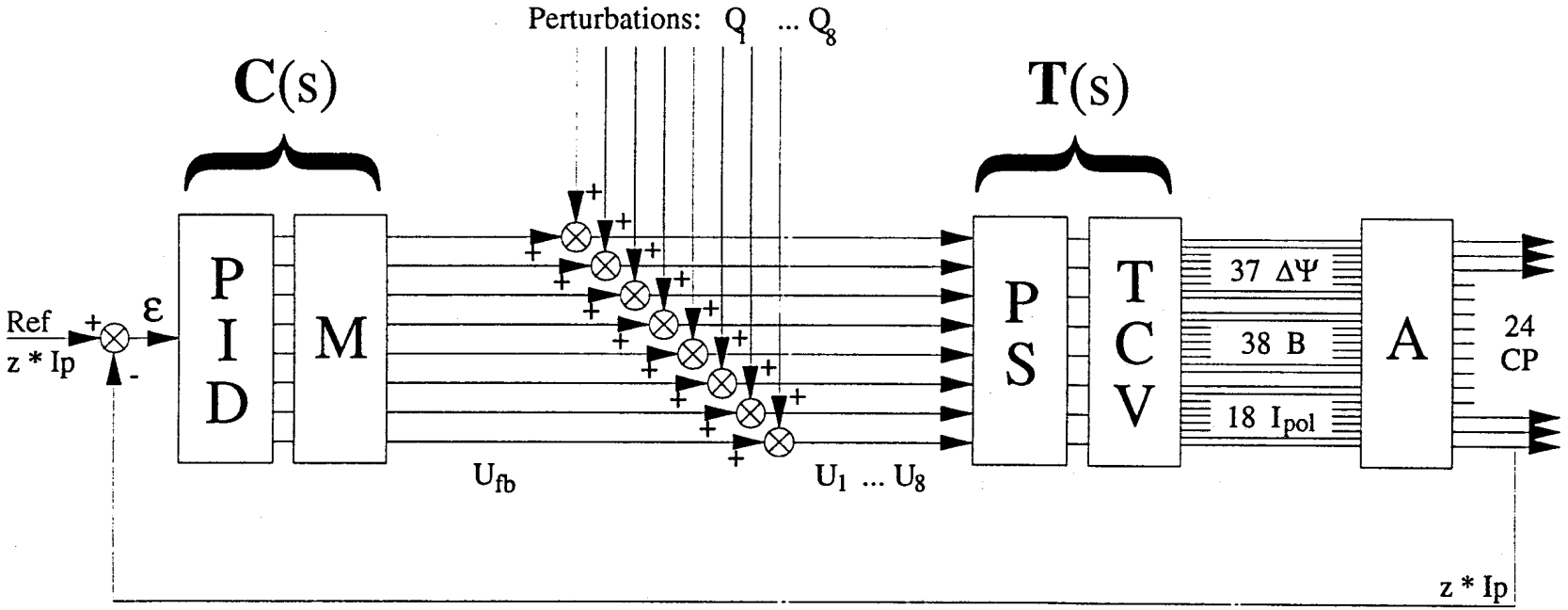

2. Simple figure of the vertical position feedback control loop, showing the 8 anti-symmetric voltage demand signals (**U**) and perturbation inputs (**Q**). The transfer functions of the SIMO feedback controller, **C**(s), and that of the MISO comprising power supplies (PS) plus plasma-vessel-coil system, **T**(s), are also indicated.

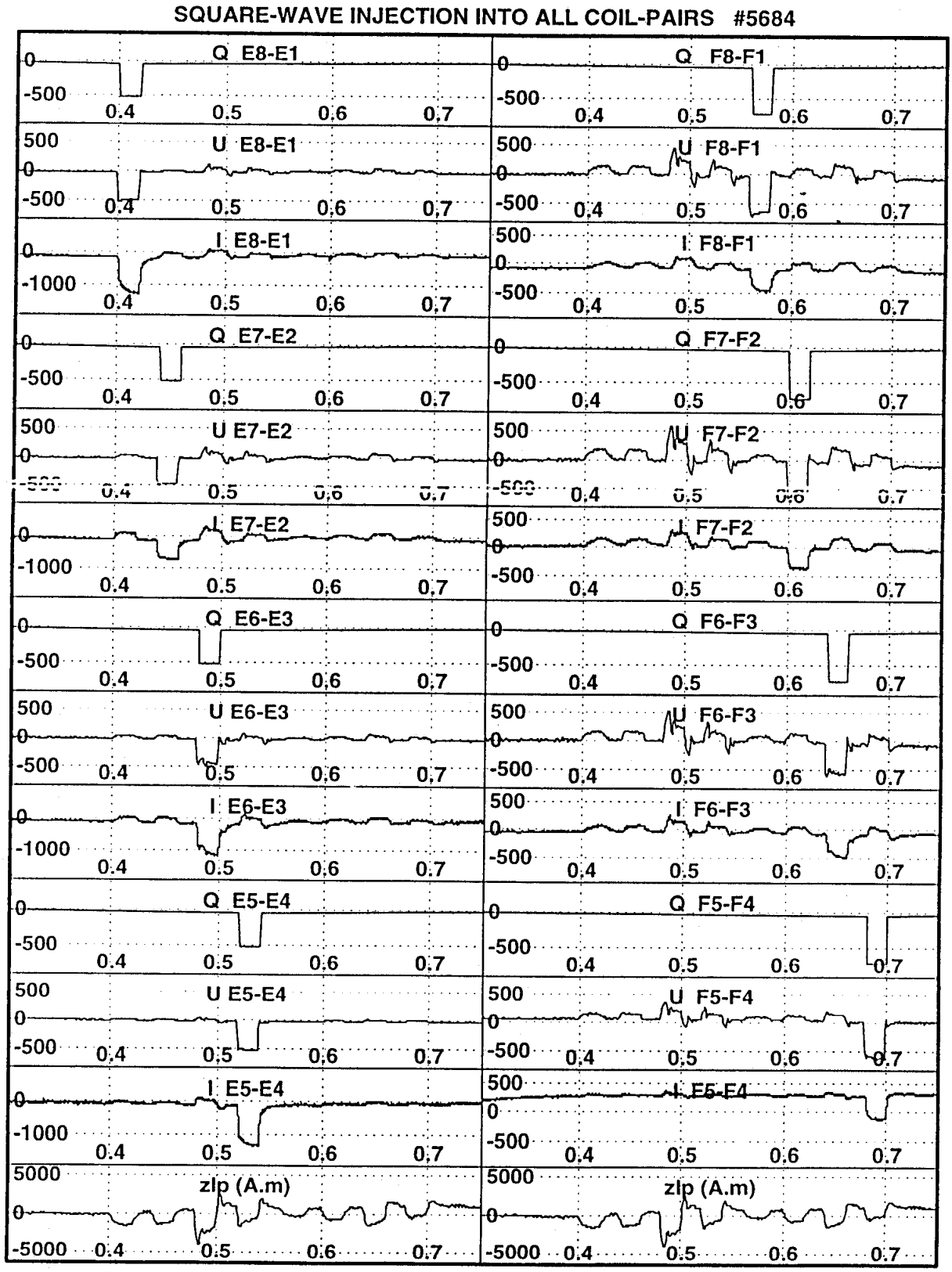

3. Response of the system to square-wave pulse injection. For each anti-symmetric coil-pair we show the perturbation (Q), the voltage demand (U) and the coil-pair current (I). The vertical position zI_p is also shown.

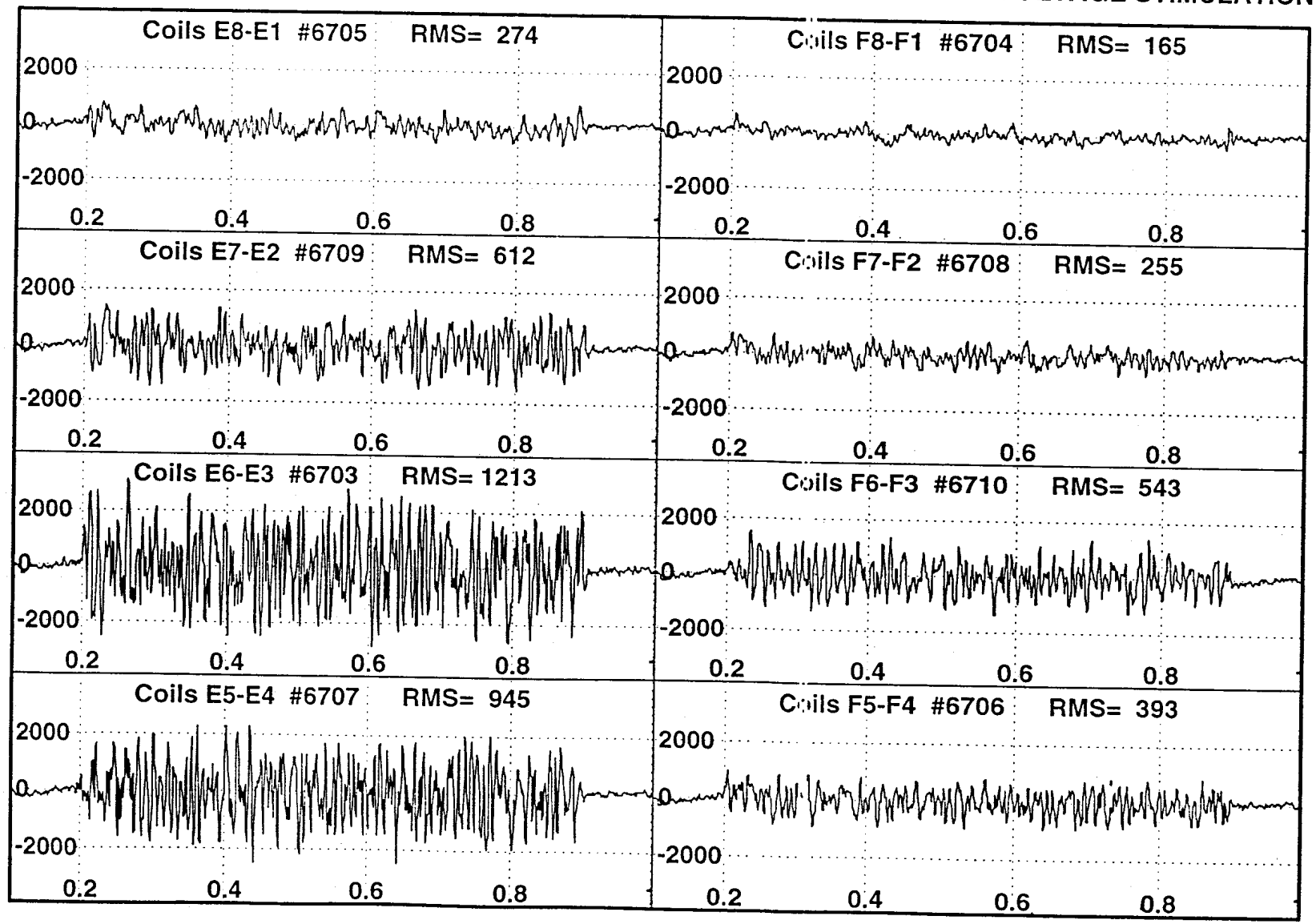

4. Plasma position response to 700 msec. of continuous anti-symmetric excitation by a random binary sequence for each of the 8 TCV coil-pairs. The variation of the current-weighted vertical plasma position response is indicated for each coil-pair (RMS).

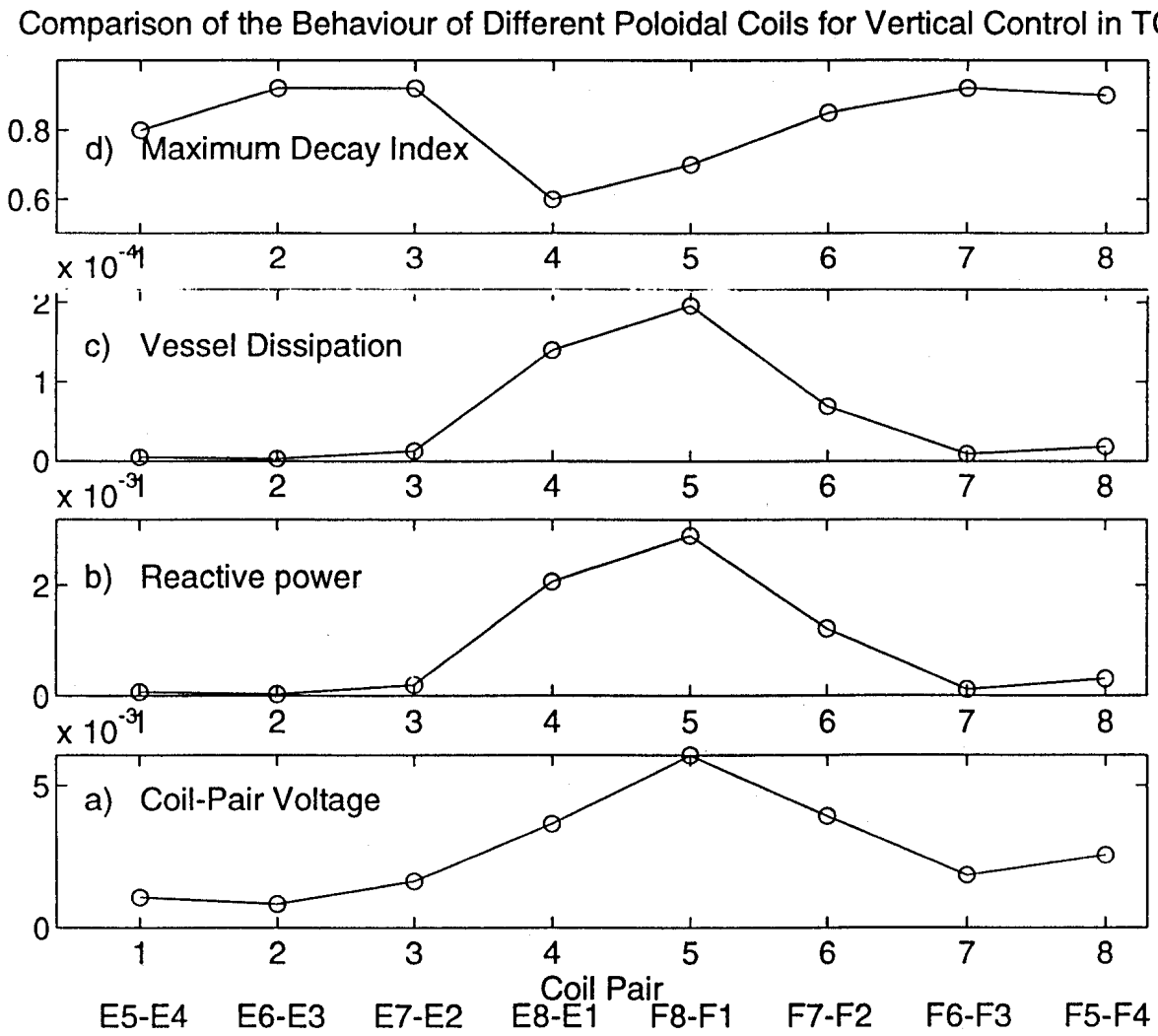

5. The response of TCV to random continuous anti-symmetric perturbation of different coil-pairs. The coils are ordered according to their poloidal position, Fig. 1. a) standard deviation of the vertical position response; b) Reactive power for unit modulation; c) Total ohmic dissipation in the vessel; d) Maximum field curvature for which the RCDM predicts vertical stabilisation using only that coil-pair, expressed as α/α_{crit}.

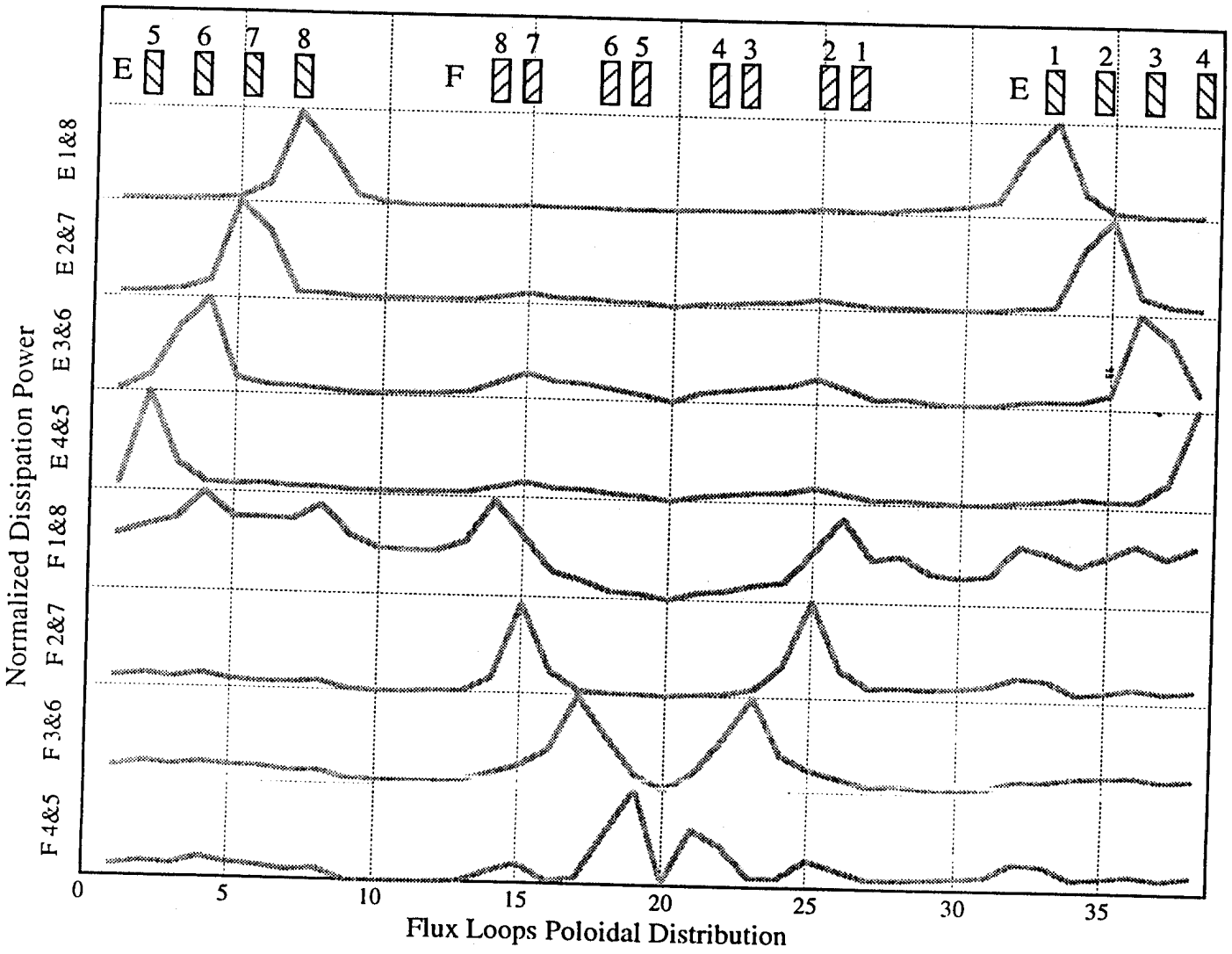

6. Measured poloidal distribution of the induced vessel currents during the square-wave injection.

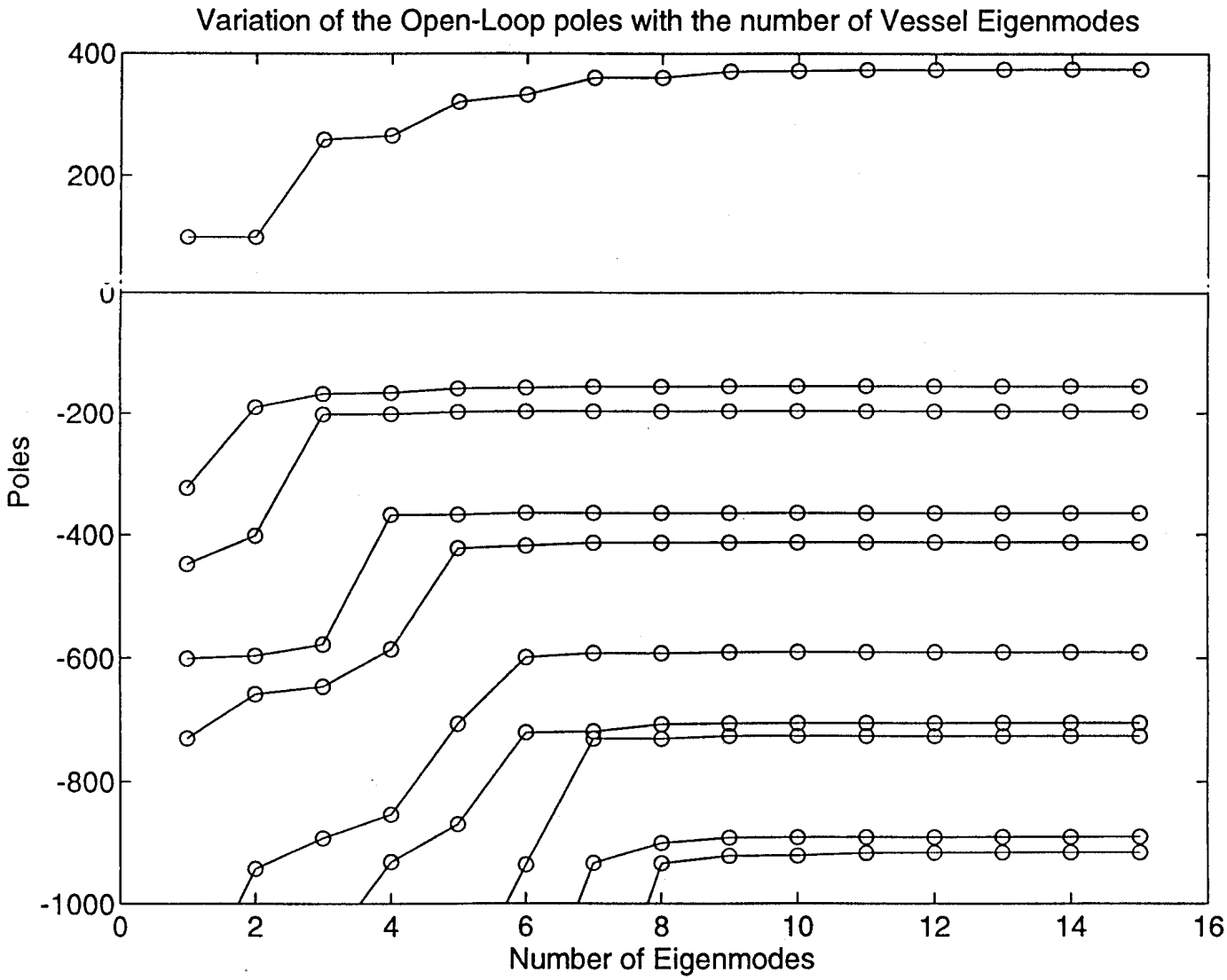

7. Evolution of the real open-loop poles as the number of eigenmodes in the vessel description is increased. Adding up-down symmetric eigenmodes to the centred plasma used in the model does not change the system response, explaining the step-wise evolution of the poles.

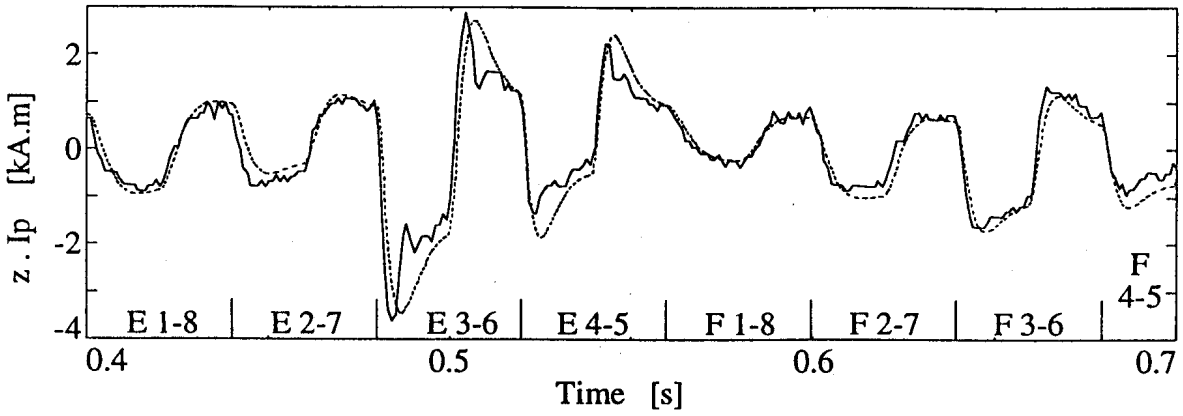

8. Comparison between the experimental square-wave response (solid line) and the modelled square-wave response (dotted-dashed line) of the zI_p position.

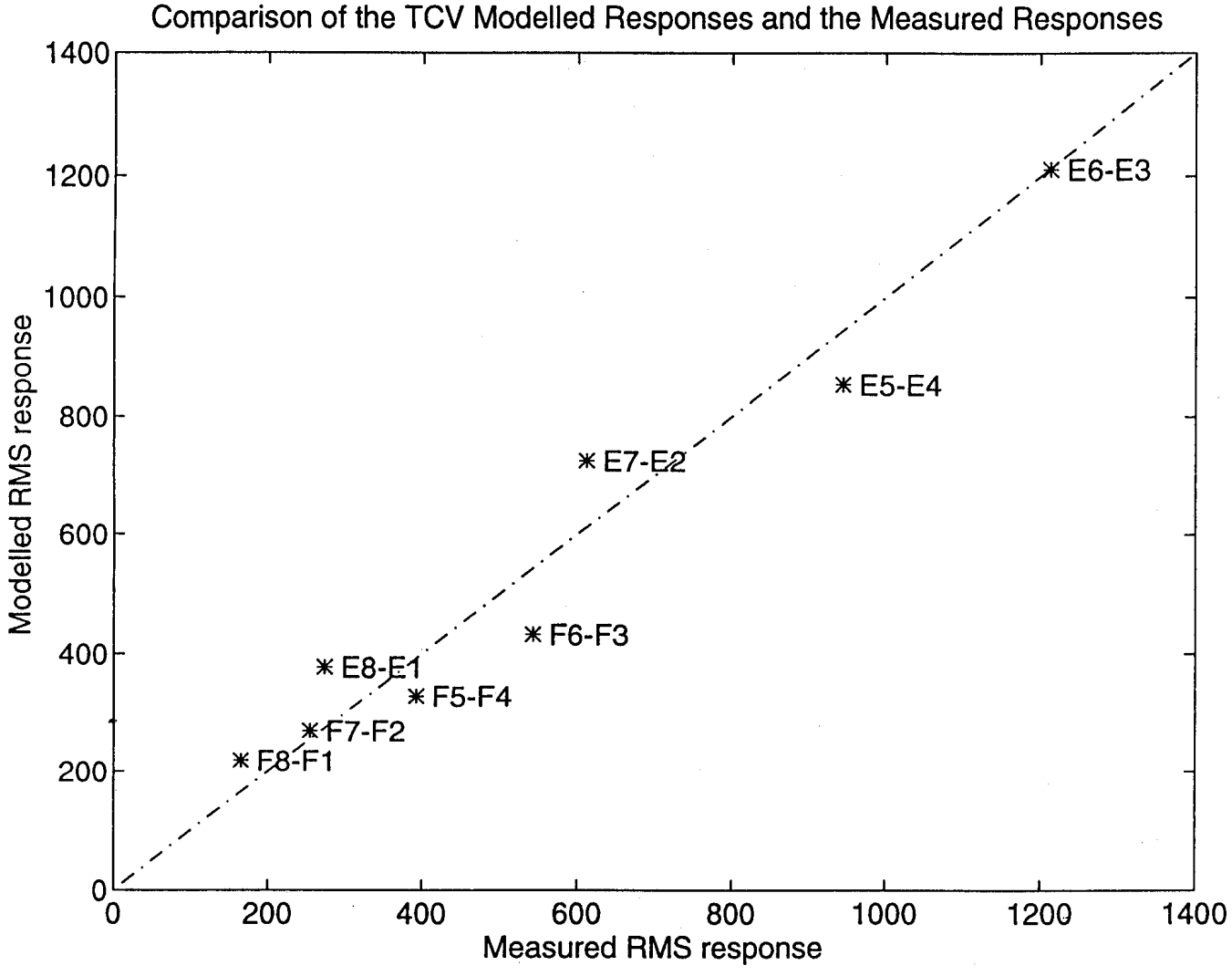

9. Comparison between the modelled and measured $\sigma(zI_p)$ position responses for the eight coil-pairs.